© 2017. Published by The Company of Biologists Ltd | Journal of Experimental Biology (2017) 220, 3062-3071 doi:10.1242/jeb.156513

RESEARCH ARTICLE

Performance, morphology and control of power-amplified mandibles in the trap-jaw ant *Myrmoteras* (Hymenoptera: Formicidae)

Fredrick J. Larabee[1,2,*], Wulfila Gronenberg[3] and Andrew V. Suarez[2,4,5]

ABSTRACT

Trap-jaw ants are characterized by high-speed mandibles used for prey capture and defense. Power-amplified mandibles have independently evolved at least four times among ants, with each lineage using different structures as a latch, spring and trigger. We examined two species from the genus *Myrmoteras* (subfamily Formicinae), whose morphology is unique among trap-jaw ant lineages, and describe the performance characteristics, spring-loading mechanism and neuronal control of *Myrmoteras* strikes. Like other trap-jaw ants, *Myrmoteras* latch their jaws open while the large closer muscle loads potential energy in a spring. The latch differs from other lineages and is likely formed by the co-contraction of the mandible opener and closer muscles. The cuticle of the posterior margin of the head serves as a spring, and is deformed by approximately 6% prior to a strike. The mandibles are likely unlatched by a subgroup of closer muscle fibers with particularly short sarcomeres. These fast fibers are controlled by two large motor neurons whose dendrites overlap with terminals of large sensory neurons originating from labral trigger hairs. Upon stimulation of the trigger hairs, the mandibles shut in as little as 0.5 ms and at peak velocities that are comparable with other trap-jaw ants, but with much slower acceleration. The estimated power output of the mandible strike (21 kW kg^{-1}) confirms that *Myrmoteras* jaws are indeed power amplified. However, the power output of *Myrmoteras* mandibles is significantly lower than distantly related trap-jaw ants using different spring-loading mechanisms, indicating a relationship between power-amplification mechanism and performance.

KEY WORDS: Biomechanics, MicroCT, Power amplification, Predation

INTRODUCTION

Speed is a fundamental performance trait and has a large impact on individual fitness by influencing predator–prey interactions (Walker et al., 2005; Watkins, 1996), dispersal distance (Fisher, 2005) and even mating success (Parsons, 1974). The speed of most animal appendages is determined by the intrinsic power limit of the muscles that generate those movements (Josephson, 1993). However, many animals have overcome these constraints by incorporating latches and elastic elements into their appendage systems and amplifying the power output of their muscles. Spring-loading legs, mouthparts and other body parts allow animals to amplify muscle power output, building up potential energy over the course of seconds or longer, and releasing it in milliseconds (Gronenberg, 1996a; Higham and Irschick, 2013; Patek et al., 2011). Power amplification is used extensively by ambush predators to catch prey and by escaping prey to generate very large accelerations to avoid being caught. Among the champions of power-amplified movements are the 'trap-jaw' ants, which generate some of the highest-velocity appendage movements ever recorded for an animal (Patek et al., 2006; Spagna et al., 2008).

Considering the diversity and ecological dominance of ants, it is not surprising that they have evolved power amplification. It is remarkable, however, that in a single insect family, trap-jaw mandibles have evolved independently at least four times for predation and defense (reviewed in Larabee and Suarez, 2014). All trap-jaw ant lineages use a similar catapult mechanism, but have adapted different structures to act as the latch, spring and trigger. Ants in the genera *Strumigenys* and *Daceton* (subfamily Myrmicinae), for example, have specialized labra that block and release the mandibles (Gronenberg, 1996b). A second lineage of trap-jaw ants in the subfamily Myrmicinae (the genus *Acanthognathus*) use specialized accessory processes at the base of the mandibles to lock them open and a modified closer muscle that releases a strike (Gronenberg et al., 1998a). Trap-jaw ants in the genera *Anochetus* and *Odontomachus* (subfamily Ponerinae) have a modified mandible insertion that locks the jaws open during muscle loading, and a specialized fast trigger muscle that unlocks the mandibles from the joint and allows them to close (Gronenberg, 1995a,b). Given their extreme performance and morphological diversity, trap-jaw ants are an excellent system for examining the convergent evolution of complex morphological adaptations and the relationship between power-amplification mechanisms and performance.

Relating different power-amplification strategies to performance output in ants is currently limited by gaps in our understanding of mandible morphology and strike kinematics for several important lineages, particularly the genus *Myrmoteras*. This relatively small genus [41 species (www.antcat.org)] is the only lineage of trap-jaw ants in the subfamily Formicinae, and their ecology and behavior are poorly understood. They display a combination of traits that are similar to other trap-jaw ants, but it is unclear how, or even if, their mouthparts are power amplified. Like other trap-jaw ants, they have long thin mandibles that are equipped with well-developed teeth along the inner margin and can be opened much wider than is the case in other trap-jaw ant genera, to 280 deg (Fig. 1). Their

[1]Department of Entomology, National Museum of Natural History, Smithsonian Institution, Washington, DC 20560, USA. [2]Department of Entomology, University of Illinois, Urbana-Champaign, Urbana, IL 61801, USA. [3]Department of Neuroscience, University of Arizona, Tucson, AZ 85721, USA. [4]Department of Animal Biology, University of Illinois, Urbana-Champaign, Urbana, IL 61801, USA. [5]Beckman Institute for Advanced Science and Technology, University of Illinois, Urbana-Champaign, Urbana 61801, IL, USA.

*Author for correspondence (larabeef@si.edu)

F.J.L., 0000-0001-8404-0146

Received 12 January 2017; Accepted 12 June 2017

Journal of Experimental Biology

Journal of Experimental Biology (2017) 220, 3062-3071 doi:10.1242/jeb.156513

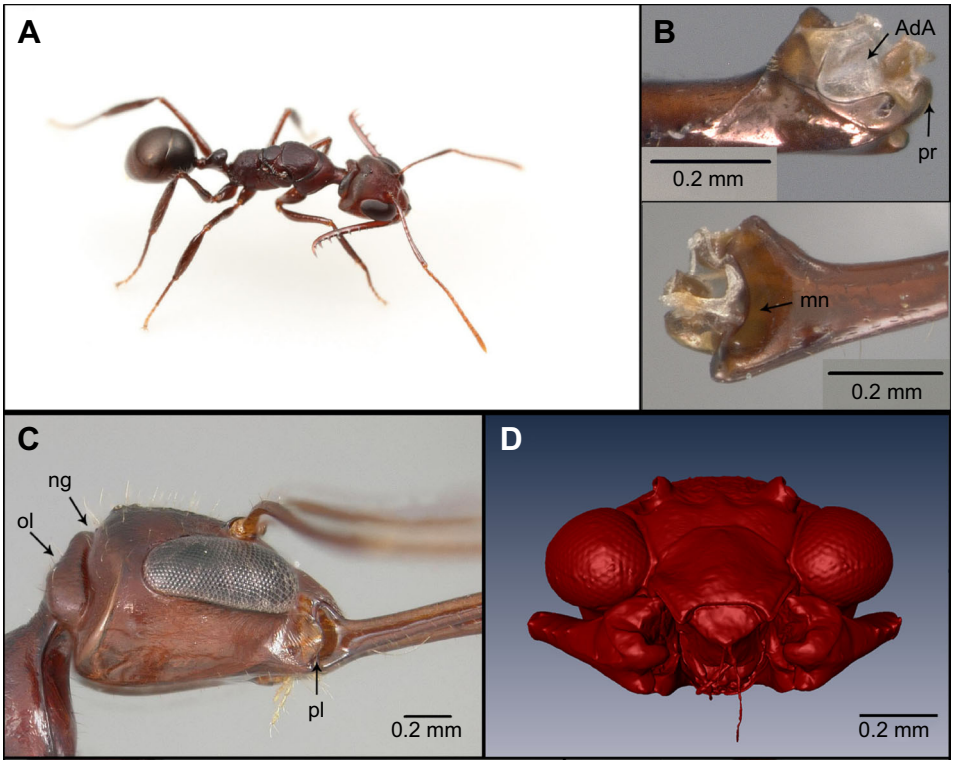

Fig. 1. Photomicrographs of *Myrmoteras iriodum* external morphology. (A) Individuals forage with mandibles open in preparation for a strike. ©Alex Wild; used with permission. (B) Mandible base with medial (top) and lateral (bottom) view illustrating the dorsal sheet portion of the closer muscle apodeme (AdA), mediobasal process (pr) and mandibular notch (mn). (C) Lateral view of the head, showing the occipital lobe (ol) and pleurostoma (pl) near the mandible joint. ng, nuchal groove. (D) Surface model of a frontal view of the head with mandibles in the open position.

mandibles are particularly long, yet slender and spiny, compared with most other trap-jaw ants, suggesting that they are not used to stun but to rapidly impale and hold prey. Also, the head of *Myrmoteras* is modified to accommodate a large mandible closer muscle that could power the mandible strike (Paul, 2001). Finally, their diet is similar to other predators with power-amplified mouthparts, consisting mostly of fast escaping prey, such as Collembolans (Moffett, 1985, 1986), suggestive that they may have convergently evolved latch, spring and trigger structures to power very fast mandible movements. Given the uncertainty of the functional morphology of their mouthparts and their distant phylogenetic relationship to other trap-jaw ants, examining *Myrmoteras* morphology and mandible performance could contribute to a better understanding of how power amplification has convergently evolved in ants.

The aim of the present study was to examine the kinematic performance, morphology and control of *Myrmoteras* trap jaws and better understand the repeated evolution of spring-loaded mandibles in ants. Specifically, we addressed three questions about the mandible mechanism of *Myrmoteras*. First, how fast are *Myrmoteras* mandibles and are they spring loaded? Second, what is the internal morphology of the mandible mechanism and, in particular, what are the latch, spring and trigger structures and the neural tissue that control mandible movement? Finally, how does the performance output of *Myrmoteras* strikes compare with other trap-jaw ant lineages whose strike performance has been studied?

MATERIALS AND METHODS

Study organism

Two colonies of *Myrmoteras barbouri* (Creighton, 1930) and two colonies of *Myrmoteras iriodum* (Moffett, 1985) were collected from Maliau Basin Conservation Area, in Sabah, Malaysia in August 2014. Colonies ranged from 10 to 25 workers and three included queens. In the lab, artificial nests were kept in plastic boxes coated with Fluon (Northern Products, Woonsocket, RI, USA), and plaster-filled Petri dishes served as nest chambers. Ants were given water and sugar *ad libitum* and fed live termites or frozen crickets three times a week. All colonies were kept at 25°C and a 12 h:12 h light:dark cycle.

High-speed videography

High-speed videography was used to visualize the loading phase of mandible strikes and to measure strike performance for workers of *M. barbouri* and *M. iriodum*. Ants were restrained to the end of a #3 insect pin on the dorsal surface of the head with dental wax (Kerr Laboratory Products, Orange, CA, USA). Care was taken to avoid gluing any part of the posterior portion of the head or anywhere on the occipital lobe. The pin was fitted onto a micromanipulator and mandible strikes were elicited with gentle puffs of air. Strikes were filmed with one of two camera arrangements. To record the loading phase of the snap, ants were filmed at 1000 frames s^{-1} with a 512-PCI camera (Photron, San Diego, CA, USA) with an MP-E 65 mm macro lens (Canon USA, Melville, NY, USA). To measure the kinematics of the mandibles during a strike, the ants were magnified with a SteREO Discovery V20 stereomicroscope (Zeiss Oberkochen, Germany) and backlit with an LED light (Visual Instrumentation Corp., Lancaster, CA, USA). Magnified trap-jaw strikes were recorded with a Phantom v9.1 high-speed camera (Vision Research Inc., Wayne, NJ, USA) with frame rates between 2×10^4 and 6×10^4 frames s^{-1} and a shutter speed of 2 µs.

Ants were frozen at −20°C to prevent drying and their wet mass was recorded within 1 week of filming. Additionally, the wet mass of each mandible, head width and length, and mandible length were recorded. Linear measurements were made with a Semprex Micro-DRO digital stage micrometer (Semprex Corp., Campbell, CA, USA) connected to a Leica MZ 12.5 stereomicroscope. Masses were measured with a UMX2 microbalance (Mettler-Toledo, Leicester, UK).

For analyzing strike kinematics, seven individuals (three *M. barbouri* and four *M. iriodum*) were filmed and 3–6 strikes were recorded from each individual. Strike trajectories were digitized

in ImageJ by tracking the x–y coordinates of the distal tip of each mandible throughout the strike. The angular displacement of the mandible, θ, was calculated from the x–y coordinate data and length of the mandible, r. Cumulative displacement was fitted with a quintic spline using the Pspline package in R v3.2.2 (http://www.R-project.org/), and instantaneous angular velocity, ω, and acceleration, α, were calculated as the first and second derivatives of the curve-fit displacement data, respectively. Linear velocity and acceleration were calculated by multiplying angular data by mandible length.

To calculate the average mass-specific muscle power required to produce the observed mandible accelerations, each mandible was modeled as a uniform rod rotating about a fixed point at its end with a moment of inertia, I:

$$I = \frac{1}{3}mr^2, \quad (1)$$

where m is the mass of the mandible and r is mandible length. The kinetic energy of the mandible, E_k, was calculated as:

$$E_k = \frac{1}{2}I\omega^2, \quad (2)$$

where ω is the maximum angular velocity of the mandible. The average mass-specific power, P, was then calculated as:

$$P = \frac{E_{k,max}}{t_{E,max}M_{adduct}}, \quad (3)$$

taking $E_{k,max}$ as the maximum kinetic energy of the mandible during the strike, $t_{E,max}$ as the time it takes to reach the maximum kinetic energy and M_{adduct} as the estimated mass of the mandible closer muscle. The mandible closer muscle was estimated as one-half of wet head mass. This is an overestimate of the muscle mass, but results in a conservative estimate of the mass-specific power required for the mandible strike.

Maximum individual performance was measured for each kinematic parameter and was calculated from the videos recorded for each individual. Strike performance was compared with published values for two other species of trap-jaw ant: *Odontomachus chelifer* and *Odontomachus ruginodis* (Spagna et al., 2008).

Microtomography

X-ray microtomography (microCT) and stereomicroscopy were used to examine the internal and external morphology, respectively, of the mandible apparatus of *M. iriodum*. MicroCT allows efficient and non-destructive imaging of internal organization of muscles as well as 3D reconstruction of biological structures (Metscher, 2009). Two sample preparations were scanned with microCT: one with closed jaws and one with jaws held open with nylon thread prior to fixation. Ants were fixed in alcoholic Bouin's solution for 2 days, gradually dehydrated in an ethanol series (70, 80, 90, 95, 100 and 100% with 20 min between changes) and finally critical-point dried. Heads were affixed to wooden dowels with low-melting-point dental wax (Kerr Laboratory Products). MicroCT was performed with an Xradia MicroXCT-400 (Carl Zeiss X-ray Microscopy, Inc., Pleasanton, CA, USA) at the Imaging Technology Group at the Beckman Institute (University of Illinois, Urbana-Champaign, IL, USA). The voltage and power of the X-ray beam were set to 40 keV and 4 W, respectively. Specimens were rotated 180 deg, with images taken every 0.25 deg. Between 720 and 745 projections were acquired with a 10× objective (exposure 10–15 s image^{-1}) while rotating the specimen 180 deg. Tomographic reconstruction was performed in XMReconstructor 8.1, and resulted in image stacks with voxel sizes of 1.87 µm (closed mandibles) and 2.04 µm (open mandibles). Volume renderings, cross-sections and surface models were produced in Amira 5.5.0 (FEI, Hillsboro, OR, USA). Image stacks of microCT scans have been uploaded to MorphoSource (www.morphosource.org).

Histology

To reveal the striation pattern and innervation of the mandible closer muscle, the mandibles, antennae and small parts of the head cuticle were removed and the heads were then fixed in 4% buffered formaldehyde for 24 h, repeatedly rinsed in phosphate buffer, impregnated with 1% osmium tetroxide solution for 6 h at 4°C, rinsed, dehydrated in dimethoxypropane, embedded in Spurr's medium (Electron Microscopy Sciences, Hatfield, PA, USA) via acetone, polymerized, and sectioned at 15 µm. To stain motor neurons, a hole was poked through the head cuticle and a small crystal of a fluorescent tracer (Fluoro Ruby, Molecular Probes, Eugene, OR, USA) was placed into the closer muscle using a minuten pin. The hole in the head capsule was then sealed and the dye was allowed to be retrogradely transported by the damaged neurons into the central nervous system overnight. To label sensory axons, the long trigger hairs on the labrum were broken off and Fluoro Ruby was applied to their slightly damaged sockets and sealed with petrol jelly. Ants were kept overnight for anterograde tracer transport. Brains containing labeled neurons were fixed, embedded and sectioned as described above (except for osmium impregnation). Brains were photographed under an epifluorescence microscope (Zeiss Axiophot and SPOT Flex Diagnostic Instruments).

RESULTS

Mandible strike kinematics

Observations in the lab confirm that *Myrmoteras* behave like other trap-jaw ants, using their long mandibles to disable prey. When provided with termites, the ants approached with their mandibles open at an angle of 280 deg and, when in range, shut them seemingly instantaneously to smash their prey. Like other trap-jaw ants, filming jaw strikes at 1000 frames s^{-1} failed to resolve the full motion of the mandible during a strike, indicating that the mandibles shut in less than 1 ms (see Movie 1).

The entire mandible movement during a strike was resolved when filmed at frame rates above 2×10^4 frames s^{-1} (Fig. 2, Movie 2). The body mass of *M. iriodum* was 60% larger than *M. barbouri* (Welch's t-test: $P<0.001$), but there was no difference in minimum strike duration, maximum angular velocity or average power (Welch's t-test: duration, $P=0.25$; velocity, $P=0.50$; average power, $P=0.54$) (Table 1). In the following discussion, strike performance for *M. barbouri* and *M. iriodum* are pooled. The average duration of a strike was 0.58±0.27 ms (mean±s.d.) with a minimum observed duration of 0.12 ms. The mandibles accelerated slowly through the beginning of the strike until they reached peak velocity about three quarters through the trajectory, at which point they decelerated rapidly (Fig. 2A). Peak angular velocities ranged from 9.23×10^3 rad s^{-1} to 1.41×10^4 rad s^{-1} and the estimated peak accelerations were on the order of 10^4 ***g***. There was no difference between the left and right mandible in peak angular velocity (paired t-test: $t=1.091$, d.f.=16, $P=0.291$) or acceleration (paired t-test: $t=1.594$, d.f.=16, $P=0.131$). The average mass-specific power output of the mandible strike was 21.4±7.1 kW kg^{-1}, two orders of magnitude greater than what is possible from direct muscle action (Josephson, 1993). To generate the observed power output, *Myrmoteras* is likely employing a spring-loading mechanism.

There was a significant difference in strike duration and peak angular velocity among the trap-jaw ant species tested (one-way

Journal of Experimental Biology (2017) 220, 3062-3071 doi:10.1242/jeb.156513

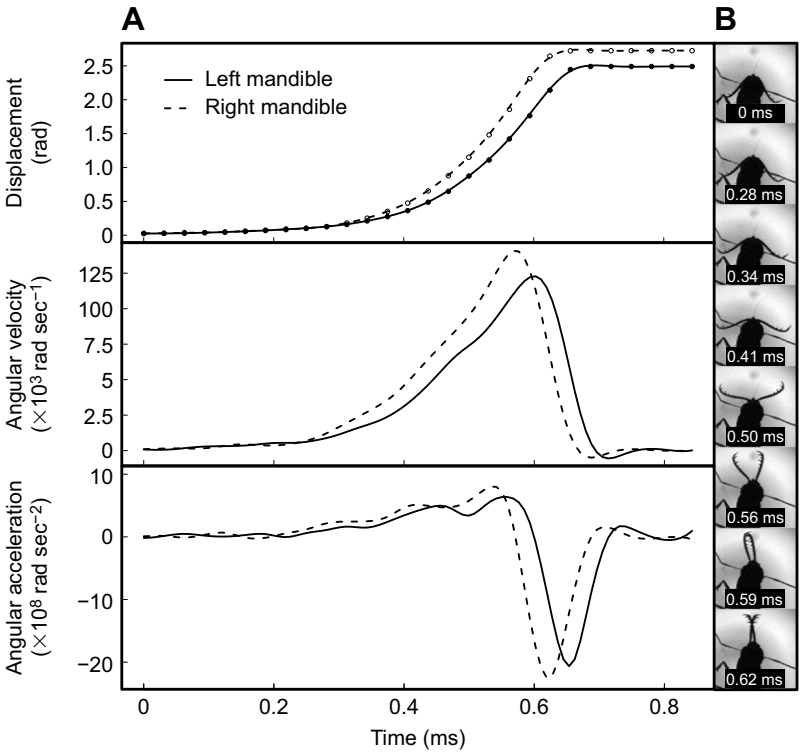

Fig. 2. Kinematics and images from high-speed videos of *M. barbouri* trap-jaw strike. (A) Kinematic profile for displacement, angular velocity and angular acceleration for the left (solid lines) and right (dashed lines) mandibles during a representative strike. In the top panel, raw displacement data calculated from the *x*–*y* coordinates of the mandible tips is shown (black and white circles) with the fitted interpolated spline overlaid. The middle and bottom panels display the first and second derivative, respectively, of that interpolated data. (B) Stills from a high-speed video (5×10^4 frames s^{-1}) resolving the mandible movement during a strike. The time (in ms) since the mandibles began moving is shown. (Also see Movie 2.)

ANOVA duration: $F_{2,13}$=11.5, P<0.001; velocity: $F_{2,13}$=123, P<0.001). *Myrmoteras* strikes were significantly longer than both the large-bodied *O. chelifer* (Tukey *post hoc* comparison: P<0.01) and the smaller, similarly sized, *O. ruginodis* (P<0.001). However, the longer strikes resulted in lower peak strike speeds only compared with *O. ruginodis* (P<0.001) (Fig. 3A). *Myrmoteras* and *O. chelifer* had peak angular velocities that were approximately half the speed of *O. ruginodis*. Unlike *Myrmoteras*, *Odontomachus* mandible strikes accelerated and decelerated very quickly. The power output of *Myrmoteras* strikes was significantly smaller than both species of *Odontomachus* (one-way ANOVA: $F_{2,13}$=58.4, P<0.001), being about one-quarter and one-tenth the amount of *O. chelifer* and *O. ruginodis*, respectively (Tukey *post hoc* comparison: versus *O. chelifer*, P=0.003; vs *O. ruginodis*, P<0.001) (Fig. 3B).

Morphology of *Myrmoteras* spring-loading apparatus

Virtual sections, volume renderings and surface models from microCT data provided visualization of the complete mouthpart apparatus of *Myrmoteras*, including external cuticular features and internal musculature (Figs 4–8, Movies 3 and 4). Visualizations from microCT were also compared with serial sections of photomicrographs from a study on glandular structures, and the general morphological features were the same (Billen et al., 2015; J. Billen, personal communication).

As stated previously, *Myrmoteras* mandibles are thin and long (approximately 1.5 times longer than the head). The mandible base is widened dorsoventrally and has a deep notch on its lateral margin that allows the mandibles to open to 280 deg (Figs 1, 5, 6). Without this notch, opening the mandibles to their full extent would be obstructed by the pleurostoma, the area of the lateral side of the head adjacent to the mandible joint. The proximal base of the mandible also has a complicated three-dimensional shape including invaginations and a prominent mediobasal process that protrudes posteriorly when the mandibles are in a closed position (Figs 1, 2, 8).

Similar to other dicondylous insects, *Myrmoteras* mandibles operate as a hinge with a single degree of freedom and are each controlled primarily by two muscles (Figs 4, 5). A large closer (adductor) muscle inserts medially on the mandible and occupies most of the dorsal and posterior volume of the head. A smaller opener (abductor) muscle inserts onto the lateral side of the mandible base and is located ventromedially. Contraction of either of these muscles causes the mandible to rotate around the axis

Table 1. Morphological and strike performance characteristics of the trap-jaw ants studied

Species	*n*	Body mass (mg)	Head width (mm)	*r* (mm)	*m* (μg)	Min. strike duration (10^{-1} ms)	ω (10^3 rad s^{-1})	α (10^8 rad s^{-2})	Max. linear velocity (m s^{-1})	Max. linear acceleration (10^5×m s^{-2})
Myrmoteras barbouri	3	1.51±0.06	1.15±0.01	1.64±0.02	24.6±1.2	4.4±0.19	12.5±0.5	5.6±2.4	20.5±0.8	9.3±4.0
Myrmoteras iriodum	4	2.50±0.19	1.40±0.03	2.01±0.02	32.0±3.6	6.0±0.28	13.3±2.7	6.4±2.9	26.7.1±5.4	12.3±6.9
Odontomachus chelifer[a]	4	24.6±2.8	2.63±0.07	2.15±0.04	310±32	2.9±0.02	17.7±3.4	4.4±1.0	39.1±9.1	8.7±2.2
Odontomachus ruginodis[a]	5	5.6±0.5	1.6±0.08	1.10±0.03	52±7	1.2±0.02	35.8±5.3	14.9±2.2	38.0±6.0	12.1±4.6

All values are means±s.d. The unit of replication (*n*) for all parameters are individual workers. The minimum or maximum values for each strike performance parameter from 3–5 strikes from each individual were used for summary statistics for each species. Variables used in kinematic calculations in the Materials and Methods are listed. [a]Values are taken from Spagna et al. (2009). α, maximum angular acceleration; ω, maximum angular velocity; *m*, mandible mass; *r*, mandible length.

Journal of Experimental Biology (2017) 220, 3062-3071 doi:10.1242/jeb.156513

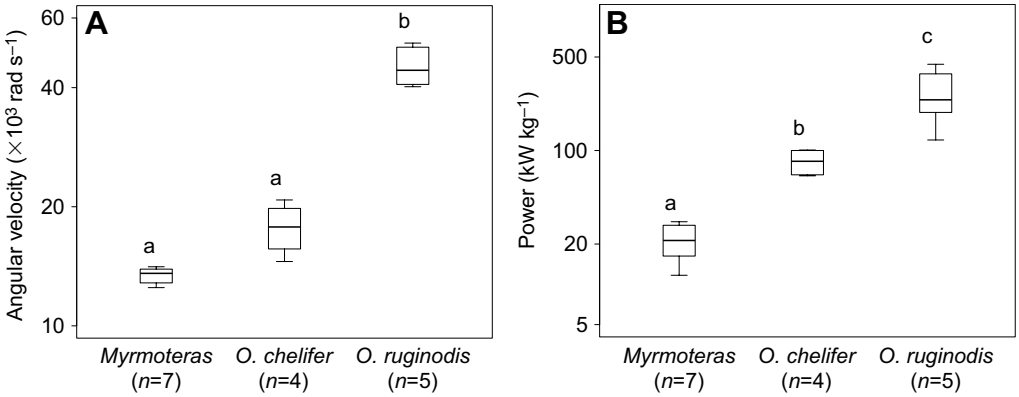

Fig. 3. Comparisons of peak angular velocity and mass-specific power for mandible strikes from three species of trap-jaw ants. Boxplots display lower and upper quartiles (rectangles), minimum and maximum values (whiskers) and sample medians (black lines). Different letters indicate means that are significantly different from each other as assessed with one-way ANOVA, $P<0.05$.

formed by the pleurostomal (dorsal) and mandibular (ventral) condyles (Fig. 1). Like in other ants, the mandible closer muscle is the largest structure in the head, filling approximately 25% of the head volume, including all of the enlarged occipital lobe on the posterior margin of the head. In contrast to the large closer muscle, the opener muscle only occupies 2.5% of the head volume. The next largest structures in the head were the brain and eyes, which take up a combined volume of 12% of the head capsule.

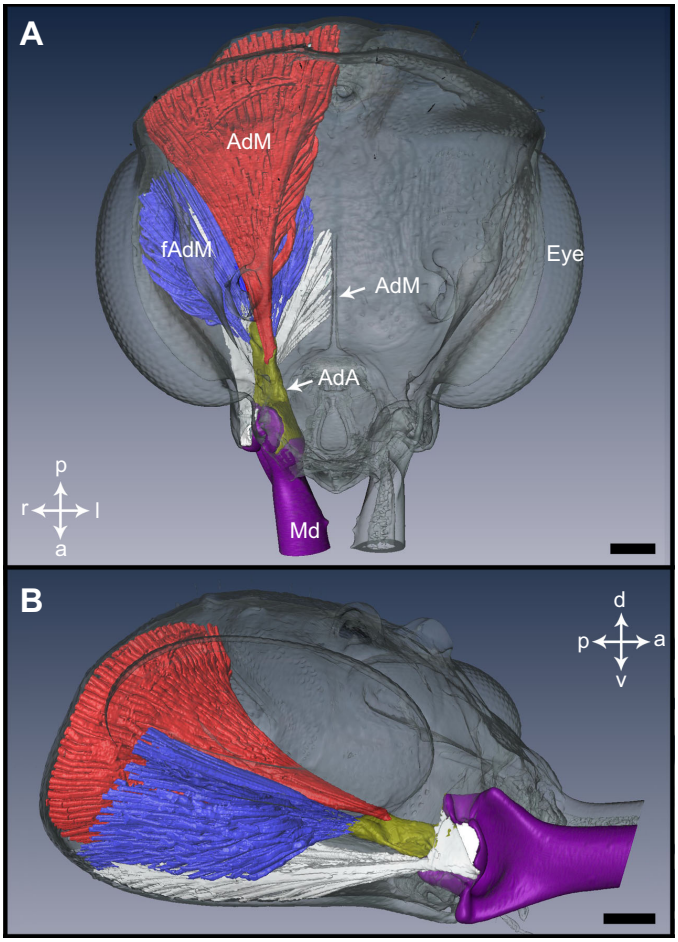

Fig. 4. General organization of the mandible apparatus of *M. iriodum*. Surface model renderings of the head, muscles and apodemes with mandibles in the closed position from X-ray microtomography data. (A) Dorsal view of head. (B) Oblique view of head. AbM, mandible opener muscle (white); AdA, closer apodeme (gold); AdM, slow mandible closer muscle (red); fAdM, fast mandible closer muscle (blue); Md, mandible (purple). Crossed arrows give the orientation of the model: a, anterior; d, dorsal; l, left; p, posterior; r, right; v, ventral. Scale bars: 100 µm.

The muscles are connected to the mandible by apodemes, highly sclerotized cuticular tissue that acts similar to the vertebrate tendon. The mandible closer (adductor) apodeme attaches broadly to the medial side of the mandible base, as a thin sheet dorsally and as a thick fiber on the mediobasal process (Figs 1, 6, 7). The main body of the apodeme is a thick, heavily sclerotized fiber approximately 50 µm in diameter. The posterior part of the apodeme base is funnel shaped and receives multiple fibrous attachments of the closer muscle (Figs 5, 7). When the mandibles are in the open position, the thin sheet of the closer apodeme wraps dorsally around the mandible base to the lateral side when they are in the open position (Fig. 7). The abductor (opener) apodeme attaches to the lateral base of the mandible, just proximal to the mandibular notch.

The complicated shape of the mandible base and the large opening angle of the mandible has a large impact on the relative lengths of the mandible opener and closer muscle moment arms (Fig. 7). In the open position, the line of action of the closer muscle is almost directly in line with the mandible joint pivot. The base of the mandible even has a groove that allows the closer apodeme to rest between the two condyles that form the axis of mandible rotation (Fig. 7). Consequently, the mandible closer muscle likely has a very small moment arm, the distance between the mandible joint and the line of action of the muscle force, allowing it to generate a large amount of force without much torque on the mandible. In contrast, the moment arm of the opener muscle is relatively long when the mandibles are wide open. Co-contraction of the opener and closer muscles could be responsible for locking the mandibles open prior to a strike.

The mandible closer muscle is made up of two separate muscles that differ in their attachment location, geometry and fiber composition (Figs 5–8). The ‘slow closer’ muscle originates broadly from the posterior margin of the head and is approximately four times larger than the ‘fast closer’. All the slow muscle fibers attach at a single location on the dorsal side of the closer apodeme very close to the sheet portion of the apodeme. The fast closer muscle surrounds the slow closer muscle, and originates on the ventral and lateral wall of the head capsule. The fast muscle fibers are attached to the closer apodeme via filaments along the funnel portion of its main body. The two muscles also differ greatly in the sarcomere lengths of their fibers (Fig. 8) [fast closer fibers: 2.6±0.26 µm (n=18 fibers measured); slow closer fibers: 10.3±1.4 µm (n=33 fibers measured)]. The differences in sarcomere length are highly significant (Student’s t-test: $P<10^{-14}$). In the absence of electrophysiological evidence, sarcomere length can be used as a proxy for muscle contraction speed (Gronenberg et al.,

Journal of Experimental Biology (2017) 220, 3062-3071 doi:10.1242/jeb.156513

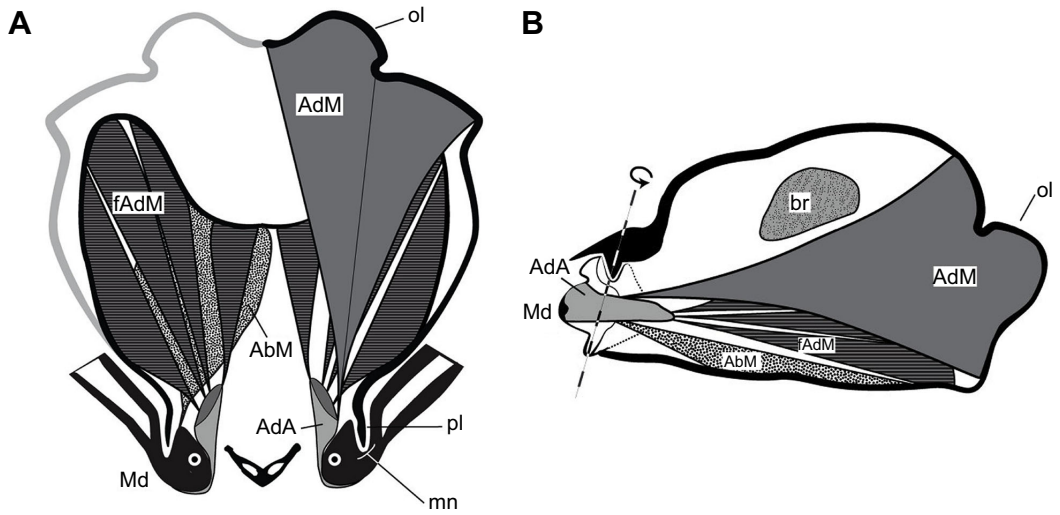

Fig. 5. Schematic of the mandible musculature in the head views of a *M. iriodum* head. (A) Dorsal view of head. The left side is sectioned approximately three quarters through the head. The right side is approximately two thirds through the head, just ventral to the eyes. (B) Sagittal section of the head through the mandible joint. AbM, mandible opener muscle; AdA, closer apodeme; AdM, slow mandible closer muscle; fAdM, fast mandible closer muscle; Md, mandible; mn, mandibular notch; ol, occipital lobe; pl, pleurostoma.

1997) and is the basis of the two closer muscle names. The fast closer fibers are comparable in sarcomere length to fast fibers described for other ants with fast mandible muscles, whereas the slow fibers have longer sarcomeres than previously described for any ant (Gronenberg et al., 1997) or, in fact, for insects in general (Nation, 2008), which would render these muscle fibers particularly slow yet forceful (Jahromi and Atwood, 1969).

While the mandibles are in the open and locked position, contraction of the slow but powerful opener muscle could load potential energy to power the mandible strike in elastic elements of the head. High-speed videos demonstrate that the posterior margin of the head, especially medially at the occipital lobe, compresses during the 5–10 s prior to a strike (Fig. 8 and Movie 1). The occipital lobe is a specialized structure on the occiput in *Myrmoteras* and is delimited by a deep groove, which we are calling the nuchal groove (Fig. 1). This groove may play an important role in energy storage for spring loading by being the site of flexion during the contraction of the slow closer muscle. By examining high-speed videos of mandible strikes, we estimated that the posterior margin of the head compresses by 6±3.0% (n=4) immediately prior to the mandible strike. The apodeme sheet that wraps around the dorsal surface of the mandible base also compresses prior to a strike (Movie 1), which may indicate that the apodeme itself might contribute to elastic energy storage, as has been suggested in other trap-jaw ants (Gronenberg, 1995a,b).

Triggering the release of the mandibles from their locked position probably depends on the fast closer muscles. These muscles attach to the posterior funnel portion of the closer apodeme, and their

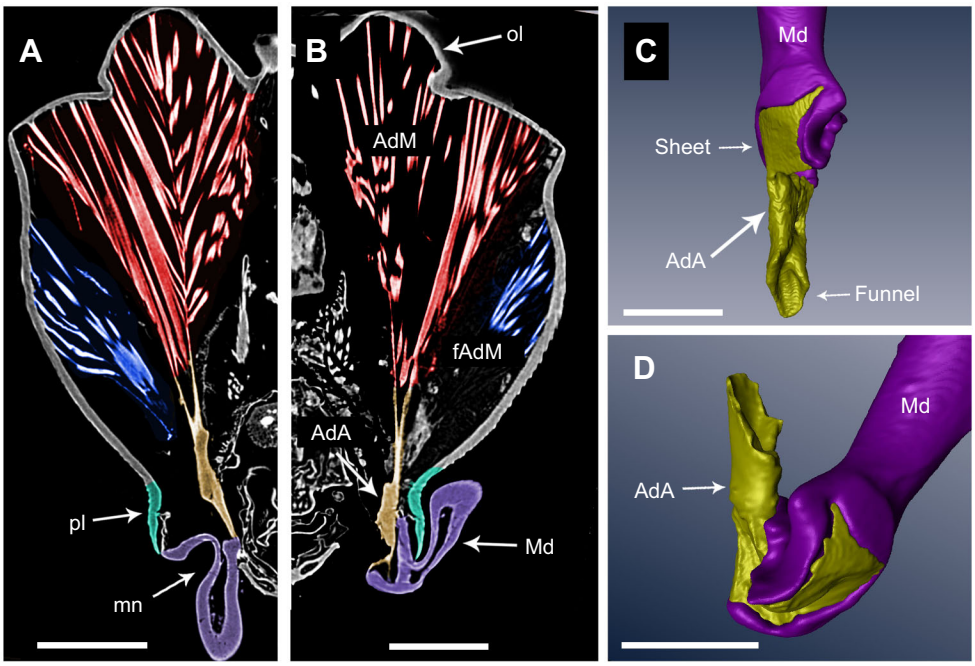

Fig. 6. Comparing the mandible apparatus in the open and closed position. (A) Virtual frontal section one third of the way through the head with mandibles in the closed position. (B) Virtual frontal section one-third of the way through the head with mandibles in the open position. (C) Surface model of the mandible and closer apodeme in the open position. (D) Surface model of the mandible and closer apodeme in the closed position. The components of the mandible are colored as in Fig. 3. AdA, closer apodeme; AdM, slow mandible closer muscle; fAdM, fast mandible closer muscle; Md, mandible; mn, mandibular notch; ol, occipital lobe; pl, pleurostoma. Scale bars: 100 μm.

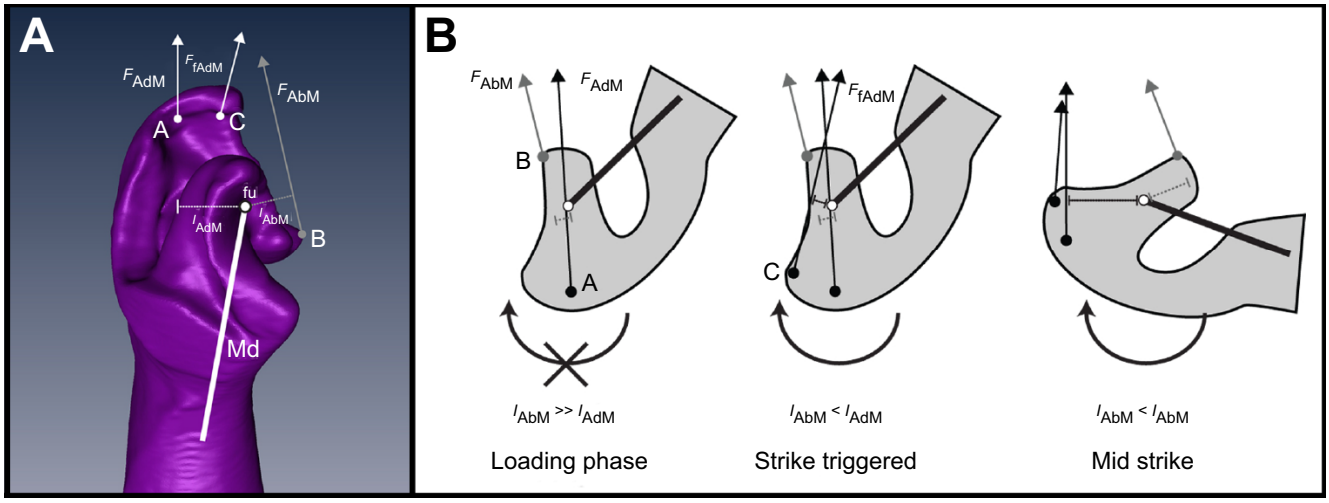

Fig. 7. Hypothesized model of *Myrmoteras* mandible mechanism. (A) Surface rendering of the mandible in the closed position from a dorsal view with labeled apodeme attachments (points A–C), moment arms (dotted lines), outlever of the mandible itself (Md) and muscle lines of action (arrows). Moment arms are illustrated as the distance from the fulcrum (fu) of the mandible perpendicular with the line of muscle action. Forces and distances of the opener muscle are illustrated in gray, and the closer muscle in white (panel A) or black (panel B). (B) Diagram of the hypothesized model of the mandible mechanism. During the loading phase of a strike, both the slow mandible closer (F_{AdM}) and opener (F_{AbM}) muscles contract, but mandible rotation is prevented because the moment arm of the slow closer muscle (l_{AdM}) is much smaller than the opener muscle (l_{AbM}). Contraction of the fast closer muscle (F_{fAdM}) changes the direction of pull on the mandible by the closer apodeme, increases the closer muscle moment arm and allows the mandibles to begin to rotate. As the mandible continues rotating, the moment arm of the closer muscle increases due to the length of the mediobasal process, and results in increased acceleration of the mandibles to quickly accelerate shut.

contraction would change the direction of pull of the closer apodeme on the mandible to be more ventrolateral and also increases the force applied to the mandible. The short sarcomeres that make up these muscle fibers indicate that they are optimized for speed (Günzel et al., 1993; Paul and Gronenberg, 1999), and would ensure that the unlatching happens rapidly.

Control of the mandible strike

Once the ant has detected prey or is otherwise prepared to strike, the mandible strike in *Myrmoteras* is triggered upon contact of the labral trigger hairs with the prey item (in the videos, the strike is released by an air puff against the trigger hairs). Deflection of a trigger hair presumably leads to the activation of a sensory neuron that supplies a remarkably thick axon (axon diameter in the labral nerve estimated from fluorescent fills: ca. 3.2 μm; Fig. 9A,B) and is thus presumably particularly fast conducting. This neuron (one on either side) provides thick, blebbed terminal collaterals in the anterior part of the subesophageal ganglion (Fig. 9B). Many of these terminals coincide with territory occupied by the dendrites (Fig. 9D) of particularly thick motor neurons (two on either side; axon diameter in nerve: 6.9 and 7.9 μm, respectively), which project through a side branch of the mandibular nerve (Fig. 9C) to supply the fast mandible closer muscle. The slow mandible closer muscle is supplied by another branch of the mandibular nerve (Fig. 9C), which does not carry any unusually large axons. Although our tracer studies did not allow us to establish synaptic connectivity, based on the surprisingly large diameter of the involved axons we propose that the thick labial sensory neurons and the thick motor neurons are synaptically connected to give rise to a particularly fast monosynaptic pathway as has been shown for the sensory-motor pathway controlling the

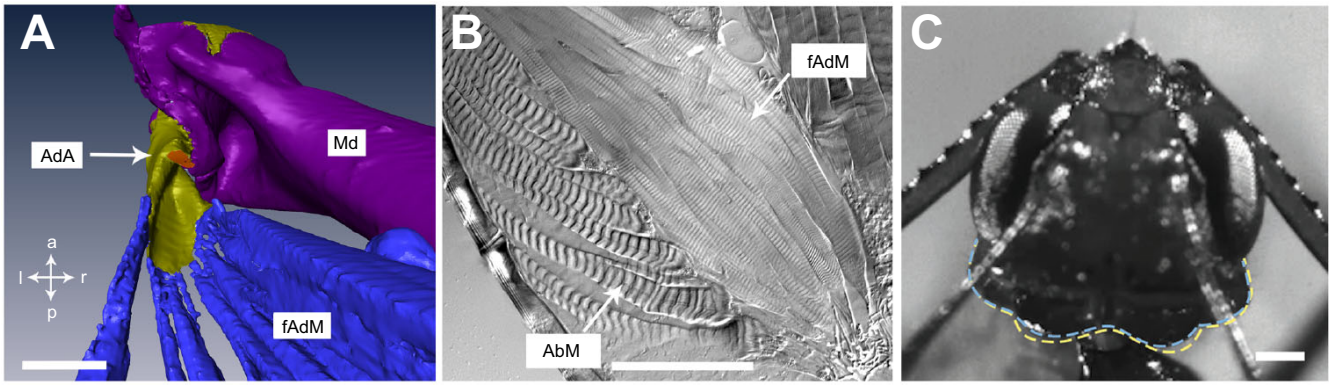

Fig. 8. Closer muscle morphology and head deformation. (A) Surface rendering of the closer apodeme (AdA) and the fast closer muscles. The slow closer muscle has been removed, but its attachment point is indicated in red. (B) Photomicrograph of the fast mandible closer muscle (fAdM) and the mandible opener muscle (AbM), illustrating the difference in sarcomere length. The fast closer muscle has significantly shorter sarcomeres, indicating a fast contraction. (C) Single frame from a high-speed video of *M. iriodum* immediately before a strike (also see Movie 1). Blue dashed line traces the amount of deformation of the occipital lobe when mandibles are fully loaded. Yellow dashed line traces the posterior margin after the strike is released. Colors correspond to the same identities listed in Fig. 4. Crossed arrows give orientation of model: a, anterior; l, left; p, posterior; r, right. Md, mandible. Scale bars: 1 mm.

Journal of Experimental Biology (2017) 220, 3062-3071 doi:10.1242/jeb.156513

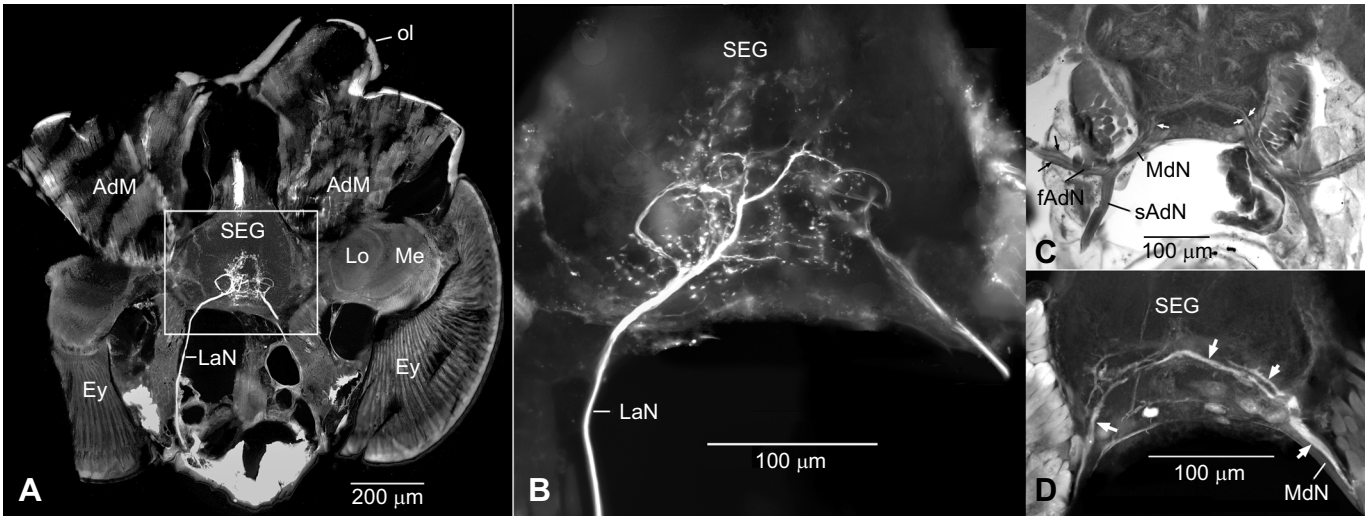

Fig. 9. Neurons underlying mandible strike control. (A) Frontal section through the head at the level of the subesophageal ganglion (SEG) showing anterogradely labeled axons originating from the labral trigger hairs projecting through the labral nerve (LaN) and terminating in the SEG. Approximate region boxed in A is enlarged in B, showing the thick sensory 'trigger' neuron and its terminals. The right half of the SEG shows additional fibers of a few smaller, 'ordinary' labral afferents. (C) Slightly larger area than the box in A of an osmium-stained section showing the mandibular nerve (MdN) bifurcating into the nerves carrying motor neurons that supply the slow (sAdN) and fast (fAdN) mandible closer muscle. Arrows point at the two large motor neuron axons on either side that control the fast closer muscle. (D) The major branches in the SEG of the same fast motor neurons (arrows) retrogradely labeled from the fast mandible closer muscle. AdM, slow mandible closer muscle; Ey, eye; Lo, lobula; Me, medulla; ol, occipital lobe.

trap-jaw reflex in the ant genus *Odontomachus* (Gronenberg, 1995b).

DISCUSSION

Proposed catapult mechanism

High-speed videography confirmed that *Myrmoteras* mandibles are spring loaded and produce much more power than can be explained by direct muscle action alone. By comparing surface renderings of *Myrmoteras* mouthparts with open and closed mandibles, we identified potential latch, spring and trigger components of the power-amplification mechanism and propose a neuronal pathway controlling the jaw strike (Fig. 8B,C). The basic catapult mechanism is similar to that found in other spring-loaded systems (Bennet-Clark, 1975; Gronenberg, 1996a; Patek et al., 2011). A latch formed from the antagonistic contraction of the mandible opener (abductor) muscle allows the slow, but powerful, closer (adductor) muscle to store potential energy in cuticular elements of the head and closer apodeme. Stimulation of the labral trigger hairs presumably activates the monosynaptic triggering pathway that causes contraction of the fast mandible closer muscle, whose shortening increases the leverage on the mandible joint and allows stored energy generated from the slow closer muscle to be applied to the mandible joint, resulting in rapid closing of the mandibles. Contraction of the fast closer muscle may be accompanied by the relaxation of the opener muscle to improve the relative moment-arm advantage of the closer muscle. Because these inferences have been made solely from morphological examination, the proposed mechanism must be considered a hypothesis until additional data from electrophysiology or additional high-speed videography can be collected.

Although the slow closer muscle generates the force required to close the mandibles, a spring is necessary to store the potential energy that is responsible for the rapid movement of the mandible strike. Based on the exceptionally large sarcomere length of its fibers (Gronenberg et al., 1997), it appears that this muscle should be extraordinarily slow contracting yet generate particularly large forces, as would be expected of a spring-loaded system. In *Myrmoteras*, several structures likely act as a spring, including the cuticle of the posterior margin of the head, which compresses in response to the contraction of the closer muscle in the seconds before a strike. The potential energy stored in the occipital lobe is passed to the mandible through the closer muscle and apodeme when the latch is released (Fig. 8). Assuming the closer muscle stays contracted for the 0.5 ms duration of a strike, the shortened muscle would be pulled by the deflected lobe and result in the rapid rotation of the mandible. Other elastic elements in the head also might play an energy storage role, including the closer apodeme and the muscle itself. Additional work will be required to determine the relative contribution of each of these elements to elastic energy storage.

The difficulty of finding *Myrmoteras* colonies in the field and the small number of individuals per colony limited the number of individuals we were able to study. As a consequence, there are several aspects of the mandible function that we could not examine, in particular the neural control and temporal activity of the mandible muscle. In other trap-jaw lineages, the large mandible closer muscle contracts slowly prior to a strike. The strike is released when trigger hairs are stimulated mechanically, which activates a fast trigger muscle responsible for unlocking the mandibles and allowing them to rotate shut (Gronenberg, 1996b; Gronenberg et al., 1998a; Just and Gronenberg, 1999). The trigger muscles are regulated by large-diameter sensory and motor neurons and form a very fast monosynaptic reflex. We assume that the same neuronal principles underlie the strike in *Myrmoteras*, and our high-speed videos and morphological examination suggest a similar mechanical scenario; however, without electrophysiological recordings of muscle activity, the temporal properties of muscle activation remain unclear.

Uncertainty in the role that trigger hairs play in activating the trap-jaw reflex also comes from comparisons with other *Myrmoteras* species. The two species that we examined, *M. barbouri* and *M. iriodum*, have well-developed labral trigger hairs, but most species (all in the subgenus *Myagroteras*) lack them (Moffett, 1985; http://antcat.org). Given the large eyes of *Myrmoteras*, visual cues may also

Journal of Experimental Biology

be involved in releasing the mandible strike. The mandible strike of *Odontomachus* trap-jaw ants can still be released when their trigger hairs are removed (Carlin and Gladstein, 1989; Mohan and Spagna, 2015). It may be that *Myrmoteras* also uses several senses to trigger their strikes.

Comparison with trap-jaw ants and other power-amplified movements

The spring-loading mechanism of *Myrmoteras* mandibles is unique among the four independent lineages of trap-jaw ant. Comparing the morphology and kinematics of these convergently evolved strategies reveals the performance consequences of different power-amplification mechanisms. For example, the unlatching mechanism of *Myrmoteras* may be responsible for the slower acceleration of its mandible strike compared with *Odontomachus* trap-jaw ants (Fig. 2). All trap-jaw lineages, including *Myrmoteras*, use muscles composed of fast contracting fibers to unlock their jaws yet slow (hence forceful) muscle fibers to power the spring mechanism (Gronenberg, 1995a, 1996b; Gronenberg et al., 1998a; Just and Gronenberg, 1999). In other lineages, however, the trigger muscle is decoupled from the function of the closer muscle, unblocking the labrum in dacetines, or removing the mandible condyle from a notch in *Anochetus* and *Odontomachus*. In *Myrmoteras*, the fast and slow closer muscles are attached to the same apodeme, and the fast closer muscle supplements the torque applied to the mandible by the slow closer muscle. Rotating the mandibles from such a large angle may partially explain why the acceleration of *Myrmoteras* mandibles is so much slower than either *O. chelifer* or *O. ruginodis*.

Similarly, differences in spring morphology may also explain some of the kinematic differences between trap-jaw lineages. *Anochetus* and *Odontomachus* store potential energy mainly in a highly sclerotized hook-shaped mandible closer apodeme (Gronenberg, 1995a). The closer apodeme of *Myrmoteras*, on the other hand, is funnel shaped, which may not have the same spring mechanics as *Odontomachus*. Additionally, the cuticle of the posterior margin of the head in *Myrmoteras* may not be as efficient a spring as the ponerine trap-jaw ant spring, owing to it being less stiff and not directly connected to the mandible. Consequently, this may be responsible for the lower peak velocities measured for *Myrmoteras* strikes. Morphological and mechanical differences in spring structures have been found to determine performance differences in other spring-loaded appendages, such as in mantis shrimp (Patek et al., 2013; Rosario and Patek, 2015).

Our kinematic data demonstrates that *Myrmoteras* mandible strikes are not on the same allometric scale as *Odontomachus*. The speed of ponerine trap-jaw strikes display a negative allometric relationship with body size (Spagna et al., 2008; F.J.L., unpublished data). There was no difference in strike performance between the two species of *Myrmoteras* we examined, despite a significant difference in body size. Compared with two species of *Odontomachus*, the minimum strike duration of *Myrmoteras* was much longer. Likewise, peak velocity in *Myrmoteras* was lower than the similarly sized *O. ruginodis*. Comparison with other trap-jaw ant genera that have been examined (*Acanthognathus*, *Daceton* or *Strumigenys*) was not possible because only maximum strike durations could be estimated for those genera (Gronenberg, 1996b; Gronenberg et al., 1998a).

The estimated power output of *Myrmoteras* strikes was approximately 21 kW kg^{-1}, which is significantly lower than other trap-jaw ants for which data is available (Fig. 3). *Odontomachus chelifer* and *O. ruginodis*, which use a different power-amplification mechanism than *Myrmoteras*, have power outputs 4 and 10 times greater than *Myrmoteras*. Other arthropods with power-amplified predatory or defensive strikes, such as trap-jaw spiders (Wood et al., 2016), smashing mantis shrimp (Patek et al., 2004) and snapping termite soldiers (Seid et al., 2008), also have between 3 and 500 times more powerful strikes than *Myrmoteras*. In contrast, the predatory strikes of *Myrmoteras* are 2 to 10 times more powerful than the power-amplified jumps of some saltatorial arthropods, such as fleas (Bennet-Clark and Lucey, 1967; Sutton and Burrows, 2011), locusts (Bennet-Clark, 1975) and springtails (Brackenbury and Hunt, 1993). In these cases, however, the jumping mechanisms are accelerating the entire body mass of the animal, rather than just a limb, resulting in the work being performed over a longer period of time (i.e. lower power output). Complicating this interpretation, however, are the exceptionally powerful jumps of flea beetles (Brackenbury and Wang, 1995) and froghoppers (Burrows, 2006), which amplify power to a similar extent as *Myrmoteras* mandible strikes.

The reduced strike performance of *Myrmoteras* may partly be explained by the function and morphology of their mandibles, which are longer and thinner compared with *Odontomachus*. *Myrmoteras* use their strikes for specialized predation of soft-bodied springtails, whose spring-loaded escape jumps occur between 10 and 50 ms after contact with a stimulus (Hopkin, 1997). This is well within the average strike duration we recorded for *Myrmoteras* strikes. In addition to catching fast and dangerous prey, the trap jaws of *Odontomachus* are also used to power escape jumps that increase their survival rate during interactions with predators (Larabee and Suarez, 2015; Patek et al., 2006; Spagna et al., 2009). The mandibles of *Odontomachus* are shorter and more robust than *Myrmoteras* jaws, likely as a result of the mechanical demands required to withstand the large accelerations and forces that power their escape jumps. *Myrmoteras* mandibles or teeth may break if they experienced equivalent accelerations or forces when closing on a hard object. Interestingly, many of the other trap-jaw ant genera have similarly thin and long mandibles (*Acanthognathus*, and many *Strumigenys* species), but probably do not typically display escape jump behavior.

The unique mandible mechanism employed by *Myrmoteras* trap-jaw ants highlights the evolutionary success of spring-loaded appendages. Trap-jaws have evolved at least four times in ants, and at least two other lineages (*Mystrium* and *Plectrotena*) employ spring-loaded 'snapping jaws' to amplify the force of their mandibles (Dejean et al., 2002; Gronenberg et al., 1998b). The repeated evolution of spring-loaded mandibles is an example of how speed has had a large impact on predator–prey interactions in terrestrial arthropod communities. Given the number of insects that employ rapid spring-loaded escape behaviors as antipredation adaptations (crickets, springtails, click-beetles), it is not surprising that a dominant predator group, such as ants, has repeatedly evolved high-performance specializations that overcome the physical limitation on predation speed.

Acknowledgements

The authors thank Brian L. Fisher for assistance in obtaining collecting and export permits for all specimens as part of Ant Course. Eli Sarnat assisted collecting ants in the field, and Josh Gibson helped film ants. The authors also thank Scott Robinson and Leilei Yin from the Beckman Institute Imaging Technology Group for assistance with microCT. Johan Billen generously shared serial photomicrographs of *Myrmoteras*. Elijah Talamas provided useful comments and discussion on Hymenoptera morphology. The manuscript was greatly improved by the comments of Philip Anderson and two anonymous reviewers.

Competing interests

The authors declare no competing or financial interests.

Journal of Experimental Biology

Author contributions

Conceptualization: F.J.L., A.V.S.; Methodology: F.J.L., W.G.; Formal analysis: F.J.L., W.G.; Investigation: F.J.L., W.G.; Resources: F.J.L., W.G., A.V.S.; Data curation: W.G., F.J.L.; Writing - original draft: F.J.L.; Writing - review & editing: F.J.L., W.G., A.V.S.; Supervision: A.V.S.; Funding acquisition: F.J.L., A.V.S., W.G.

Funding

This work was supported by the National Science Foundation (DDIG DEB-1407279 to F.J.L., IOS-1354191 to W.G.); the Smithsonian Institution (Peter Buck Fellowship to F.J.L.); the National Geographic Society (Explorers Grant 9481-14 to A.V.S.); and The School of Integrative Biology, University of Illinois, Urbana-Champaign (Graduate Fellowship to F.J.L.).

Data availability

X-ray microtomography data are available from MorphoSource: http://morphosource.org/Detail/ProjectDetail/Show/project_id/266

Supplementary information

Supplementary information available online at
http://jeb.biologists.org/lookup/doi/10.1242/jeb.156513.supplemental

References

Bennet-Clark, H. C. (1975). The energetics of the jump of the locust *Schistocerca gregaria*. *J. Exp. Biol.* **63**, 53-83.

Bennet-Clark, H. C. and Lucey, E. C. A. (1967). The jump of the flea: a study of the energetics and a model of the mechanism. *J. Exp. Biol.* **47**, 59-76.

Billen, J., Mandonx, T., Hashim, R. and Ito, F. (2015). Exocrine glands of the ant *Myrmoteras iriodium*. *Entomol. Sci.* **18**, 167-173.

Brackenbury, J. and Hunt, H. (1993). Jumping in springtails: mechanism and dynamics. *J. Zool.* **229**, 217-236.

Brackenbury, J. and Wang, R. (1995). Ballistics and visual targeting in flea-beetles (Alticinae). *J. Exp. Biol.* **198**, 1931-1942.

Burrows, M. (2006). Jumping performance of froghopper insects. *J. Exp. Biol.* **209**, 4607-4621.

Carlin, N. F. and Gladstein, D. S. (1989). The "bouncer" defense of *Odontomachus ruginodis* and other odontomachine ants (Hymenoptera: Formicidae). *Psyche* **96**, 1-19.

Creighton, W. S. (1930). A review of the genus *Myrmoteras* (Hymenoptera, Formicidae). *J. New York Entomol. S.* **38**, 177-192.

Dejean, A., Suzzoni, J.-P., Schatz, B. and Orivel, J. (2002). Territorial aggressiveness and predation: two possible origins of snapping in the ant *Plectroctena minor*. *C. R. Biol.* **325**, 819-825.

Fisher, R. (2005). Swimming speeds of larval coral reef fishes: impacts on self-recruitment and dispersal. *Mar. Ecol. Prog. Ser.* **285**, 223-232.

Gronenberg, W. (1995a). The fast mandible strike in the trap-jaw ant *Odontomachus* I. Temporal properties and morphological characteristics. *J. Comp. Physiol. A* **176**, 391-398.

Gronenberg, W. (1995b). The fast mandible strike in the trap-jaw ant *Odontomachus* II. Motor Control. *J. Comp. Physiol. A* **176**, 399-408.

Gronenberg, W. (1996a). Fast actions in small animals: springs and click mechanisms. *J. Comp. Physiol. A* **178**, 727-734.

Gronenberg, W. (1996b). The trap-jaw mechanism in the dacetine ants *Daceton armigerum* and *Strumigenys* sp. *J. Exp. Biol.* **199**, 2021-2033.

Gronenberg, W., Paul, J., Just, S. and Hölldobler, B. (1997). Mandible muscle fibers in ants: fast or powerful? *Cell Tissue Res.* **289**, 347-361.

Gronenberg, W., Brandão, C. R. F., Dietz, B. and Just, S. (1998a). Trap-jaws revisited: the mandible mechanism of the ant *Acanthognathus*. *Physiol. Entomol.* **23**, 227-240.

Gronenberg, W., Hölldobler, B. and Alpert, G. (1998b). Jaws that snap: control of mandible movements in the ant *Mystrium*. *J. Insect Physiol.* **44**, 241-253.

Günzel, D., Galler, S. and Rathmayer, W. (1993). Fibre heterogeneity in the closer and opener muscles of crayfish walking legs. *J. Exp. Biol.* **175**, 267-282.

Higham, T. E. and Irschick, D. J. (2013). Springs, steroids, and slingshots: the roles of enhancers and constraints in animal movement. *J. Comp. Physiol. B* **183**, 583-595.

Hopkin, S. P. (1997). *Biology of the Springtails: (Insecta: Collembola)*. Oxford: OUP.

Jahromi, S. S. and Atwood, H. L. (1969). Correlation of structure, speed of contraction, and total tension in fast and slow abdominal muscle fibers of the lobster (*Homarus americanus*). *J. Exp. Zool. Part A* **171**, 25-37.

Josephson, R. K. (1993). Contraction dynamics and power output of skeletal muscle. *Ann. Rev. Physiol.* **55**, 527-546.

Just, S. and Gronenberg, W. (1999). The control of mandible movements in the ant *Odontomachus*. *J. Insect Physiol.* **45**, 231-240.

Larabee, F. J. and Suarez, A. V. (2014). The evolution and functional morphology of trap-jaw ants (Hymenoptera: Formicidae). *Myrmecol. News* **20**, 25-36.

Larabee, F. J. and Suarez, A. V. (2015). Mandible-powered escape jumps in trap-jaw ants increase survival rates during predator-prey encounters. *PLoS ONE* **10**, e0124871.

Metscher, B. D. (2009). MicroCT for comparative morphology: simple staining methods allow high-contrast 3D imaging of diverse non-mineralized animal tissues. *BMC Physiol.* **9**, 1-11.

Moffett, M. W. (1985). Revision of the genus *Myrmoteras* (Hymenoptera: Formicidae). *Bull. Mus. Comp. Zool.* **151**, 1-53.

Moffett, M. W. (1986). Trap-jaw predation and other observations on two species of *Myrmoteras* (Hymenoptera: Formicidae). *Insect. Soc.* **33**, 85-99.

Mohan, V. and Spagna, J. C. (2015). Jump performance in trap-jaw ants: beyond trigger hairs. *Bull. N.J. Acad. Sci.* **60**, 1-4.

Nation, J. L. (2008). *Insect Physiology and Biochemistry*. 2nd edn. CRC Press: Boca Raton, FL.

Parsons, P. A. (1974). Male mating speed as a component of fitness in *Drosophila*. *Behav. Genet.* **4**, 395-404.

Patek, S. N., Korff, W. L. and Caldwell, R. L. (2004). Deadly strike mechanism of a mantis shrimp. *Nature* **428**, 819-820.

Patek, S. N., Baio, J. E., Fisher, B. L. and Suarez, A. V. (2006). Multifunctionality and mechanical origins: Ballistic jaw propulsion in trap-jaw ants. *Proc. Natl. Acad. Sci. USA* **103**, 12787-12792.

Patek, S. N., Dudek, D. M. and Rosario, M. V. (2011). From bouncy legs to poisoned arrows: elastic movements in invertebrates. *J. Exp. Biol.* **214**, 1973-1980.

Patek, S. N., Rosario, M. V. and Taylor, J. R. A. (2013). Comparative spring mechanics in mantis shrimp. *J. Exp. Biol.* **216**, 1317-1329.

Paul, J. (2001). Mandible movements in ants. *Comp. Biochem. Physiol. A* **131**, 7-20.

Paul, J. and Gronenberg, W. (1999). Optimizing force and velocity: mandible muscle fibre attachments in ants. *J. Exp. Biol.* **202**, 797-808.

Rosario, M. V. and Patek, S. N. (2015). Multilevel analysis of elastic morphology: the mantis shrimp's spring. *J. Morphol.* **276**, 1123-1135.

Seid, M. A., Scheffrahn, R. H. and Niven, J. E. (2008). The rapid mandible strike of a termite soldier. *Curr. Biol.* **18**, R1049-R1050.

Spagna, J. C., Vakis, A. I., Schmidt, C. A., Patek, S. N., Zhang, X., Tsutsui, N. D. and Suarez, A. V. (2008). Phylogeny, scaling, and the generation of extreme forces in trap-jaw ants. *J. Exp. Biol.* **211**, 2358-2368.

Spagna, J. C., Schelkopf, A., Carrillo, T. and Suarez, A. V. (2009). Evidence of behavioral co-option from context-dependent variation in mandible use in trap-jaw ants (*Odontomachus* spp.). *Naturwissenschaften* **96**, 243-250.

Sutton, G. P. and Burrows, M. (2011). Biomechanics of jumping in the flea. *J. Exp. Biol.* **214**, 836-847.

Walker, J. A., Ghalambor, C. K., Griset, O. L., McKenney, D. and Reznick, D. N. (2005). Do faster starts increase the probability of evading predators? *Funct. Ecol.* **19**, 808-815.

Watkins, T. B. (1996). Predator-mediated selection on burst swimming performance in tadpoles of the Pacific tree frog, *Pseudacris regilla*. *Physiol. Zool.* **69**, 154-167.

Wood, H. M., Parkinson, D. Y., Griswold, C. E. Gillespie, R. G. and Elias, D. O. (2016). Repeated evolution of power-amplified predatory strikes in trap-jaw spiders. *Curr. Biol.* **26**, 1057-1061.

SUPPLEMENTARY INFORMATION

SUPPLEMENTARY MOVIE 1. High-speed video of *Myrmoteras* mandible strike. Mandible strike recorded at 1000 frames s^{-1} to visualize deformation of the head during the loading phase of a strike.

SUPPLEMENTARY MOVIE 2. High-speed video of *Myrmoteras* mandible strike. Mandible strike recorded at $6x10^4$ frames s^{-1} to completely resolve mandible motion during a strike.

Journal of Experimental Biology • Supplementary information

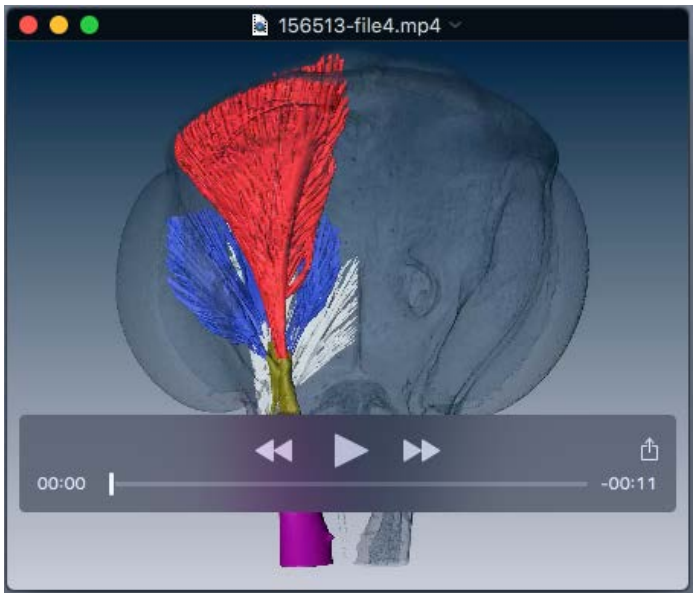

SUPPLEMENTARY MOVIE 3. Video of surface rendering of mouthpart apparatus in open position. Surface rendering from microCT data illustrating the special arrangement of the muscles, apodemes and cuticular elements of the mandible apparatus. Colors are as indicated in Fig. 3.

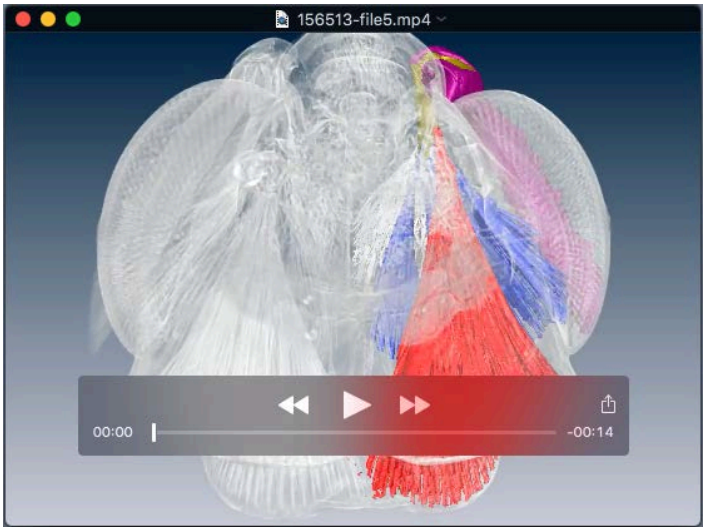

SUPPLEMENTARY MOVIE 4. Video of surface rendering of mouthpart apparatus in closed position. Surface rendering from microCT data illustrating the special arrangement of the muscles, apodemes and cuticular elements of the mandible apparatus. Colors are as indicated in Fig. 3.

Journal of Experimental Biology • Supplementary information